

## ZnS Nanocrystals as an Additive for Gamma-Irradiated Poly (Vinyl Chloride)

Roberta Cristina da Silva<sup>a</sup>, Lindomar Avelino da Silva<sup>a</sup>, Patricia Lopes Barros de Araújo<sup>a</sup>, Elmo Silvano de Araújo<sup>a</sup>, Renata Francisca da Silva Santos<sup>a</sup>, Kátia Aparecida da Silva Aquino<sup>a\*</sup>

<sup>a</sup>Laboratório de Polímeros e Nanoestruturas, Departamento de Energia Nuclear, Universidade Federal de Pernambuco, Av. Prof. Luiz Freire, 1000, 50740-545, Recife, PE, Brazil

Received: December 11, 2016; Revised: December 07, 2017; Accepted: December 08, 2017

Zinc sulfide (ZnS) was synthesized by sonochemical method and nanoparticles with crystallite size around 2 nm were obtained. PVC containing ZnS nanoparticles at concentrations of 0.10; 0.30; 0.50; 0.7 and 1.00 wt% were gamma irradiated (<sup>60</sup>Co) at room temperature in air. No appreciable decrease in PVC Viscosity-Average Molar Mass ( $M_v$ ) was observed for samples containing 0.7 wt% of ZnS nanocrystals. It was demonstrated that the addition of ZnS nanocrystals imparted molecular protection to the polymer matrix while improving flexibility, by decreasing the Young Modulus of PVC films. These results suggest the use of sonochemically synthesized ZnS nanocrystals as a new additive for radiation-grade PVC materials.

**Keywords:** Zinc sulfide nanocrystals, sonochemical synthesis, radiolytic degradation, stabilization.

### 1. Introduction

Polymer composites might present improved physical properties when compared to their polymer matrices counterparts. Thus, new combination of materials can be manufactured to meet specific requirements, which are difficult to fulfill by using a single component<sup>1</sup>.

Poly (vinyl chloride) (PVC) is a suitable polymer matrix for composites, because of its low cost, good chemical stability, and biocompatibility<sup>2</sup>. Furthermore, PVC is compatible with a wide range of additives and undergoes remarkable changes in its properties due to additivation<sup>3</sup>.

Zinc sulfide (ZnS), along with many other inorganic sulfides, exhibits a broad range of useful properties. This sulfide presents good chemical stability and physical strength, being first used as a semiconductor<sup>4,5</sup>.

Kolahi and co-workers<sup>6</sup> fabricated ZnS nanocrystals embedded in polyvinyl alcohol (PVA) matrix by wet chemical method, and observed quantum confinement effect in these nanocomposites. Ogata and collaborators<sup>7</sup> prepared polymer/ZnS nanoparticle composites by matrix-mediated synthesis and obtained homogeneously dispersed nanoparticles in the polymer, which may be useful for quantum dots and optical devices. Osuntokun and Ajibade<sup>8</sup> reported the synthesis and structural studies of ZnS and CdS nanoparticles in polyvinylpyrrolidone, PVA, and poly(methyl methacrylate) matrices. They prepared metal sulfides/polymer nanocomposites by solution casting method, with good results. Tiwari and Dhoble<sup>9</sup> reported surface passivation of ZnS nanoparticles in various polymer ligands/matrices.

Ultrasound irradiation is an effective method for inorganic nanoparticles synthesis, with advantages such as accelerating chemical reactions, enhancing mass transfer, shortening reaction cycles, improving reaction yield, altering reaction pathways, increasing surface area between the reactants, and accelerating dissolution, among others<sup>10</sup>.

The primary sonochemistry mechanism is based on acoustic cavitation, which is the formation, growth and collapse of bubbles in a liquid. Violent collapse of bubbles in less than a microsecond produces extreme heat, forming short-lived hot spots, and high pressure. These extreme transient conditions allow synthesis on the benchtop, at room-temperature conditions, in media that would otherwise require high temperatures, high pressures, or long reaction times<sup>11,12</sup>. Zinc sulfide sonochemical synthesis is a suitable preparation method, which allows fast and simple obtention of morphologically pure products<sup>13-18</sup>, circumventing tedious and laborious methods already described in the literature<sup>19,20</sup>.

PVC has applications that range from rigid pipes to electron-beam or gamma irradiation sterilizable medical devices. However, when submitted to gamma irradiation, PVC molecular structure might degrade as a result of main chain scissions and crosslinking effects<sup>21,22</sup>.

In this paper, we present sonochemically synthesized ZnS nanocrystals as a new additive for radiation-grade PVC. Our findings suggest that ZnS nanocrystals are suitable radiostabilizers for gamma-irradiated PVC, while enables lower matrix rigidity. Our work contributes to the development of inorganic nanomaterials as active fillers for commodity polymers.

\*email: [aquino@ufpe.br](mailto:aquino@ufpe.br)

## 2. Materials and Methods

### 2.1 Synthesis and characterization of ZnS nanocrystals

All reagents used were of analytical grade. Zinc acetate hydrate ( $C_4H_6O_4Zn.H_2O$ ) (VETEC®, Brazil), thioacetamide ( $CH_3CSNH_2$ ) (Sigma Aldrich), absolute ethanol (FMAIA®, Brazil) and tetrahydrofuran (THF) (VETEC®, Brazil) were used without further purification. Methyl-ethyl-ketone (MEK) (DINAMICA®, Brazil) was dried with  $Na_2SO_4$  and purified by distillation prior to use.

A typical reaction procedure was done with 1.317g of  $C_4H_6O_4Zn.H_2O$  and 1.35g of thioacetamide dissolved in 100 ml of absolute ethanol in a 250 ml beaker. Then, ultrasonic irradiation was performed for 30 minutes with a high-intensity ultrasonic probe (Sonic, 20 kHz, 500 W) directly immersed in the reaction medium, under 100% ultrasound intensity, to form the precipitate. After the reaction, the obtained ZnS precipitate was centrifuged (Quimis centrifuge Q222TM, Relative Centrifugal Force (RCF) 2,555xg), washed successively with absolute ethanol, distilled water, and acetone, and then placed in a desiccator at room temperature until complete solvents evaporation. The final product was inspected by Scanning Electron Microscopy (SEM, Quanta 200 FEG) in gold-coated samples at a magnification of 6000x.

X-ray powder diffraction (XRD) analysis of the product was carried out with a Siemens D5000 Diffractometer, equipped with graphite monochromator (CuK $\alpha$  radiation  $\lambda = 1.5418\text{\AA}$ ) using a scanning rate of 0.02 deg/s in the  $2\theta$  range from 5° to 80°. Crystallite size was calculated according to the Debye-Scherrer formula using Equation 1<sup>19</sup>:

$$L = \frac{0.9\lambda}{B \cos\theta} \quad (1)$$

where L is the coherence length, B is the full width at half maximum of the diffraction peak unit,  $\lambda$  is the wavelength of the X-ray radiation, and  $\theta$  is the Bragg angle of the diffraction peak.

Energy Dispersive Spectroscopy (EDS) experiments and Transmission Electron Microscopy (TEM) images were obtained using a G 200 microscope (FEI Tecnai 20, USA) operating at 200 kV, in bright field mode. All samples were prepared by dripping a small amount of a diluted ethanol suspension atop a 400 mesh carbon-coated copper grid and allowing the solvent to evaporate.

### 2.2 Preparation of PVC films

Additive-free PVC (BRASKEM, Brazil) was used as supplied. PVC and PVC with ZnS (PVC/ZnS) films were prepared by solvent-casting from MEK solvent by slow evaporation in air at room temperature ( $\approx 27^\circ\text{C}$ ). Concentrations of ZnS nanocrystals used in this study were 0.10; 0.30; 0.50; 0.7 and 1.00 wt%. Films were characterized

by Scanning Electron Microscopy (SEM, Quanta 200FEG) in gold-coated samples.

### 2.3 Viscosity measurements

Cinematic viscosity of PVC and PVC/ZnS THF solutions were carried using an Anton Paar SVM 3000 Stabinger Viscometer. Viscosity results were obtained from the Equations showed in Table 1. Viscosity Average Molar Mass ( $M_v$ ) was calculated from the corresponding  $[\eta]$  values through Mark-Houwink Equation<sup>23</sup> (Equation 2).

$$[\eta] = KM_v^a \quad (2)$$

where K and a are  $1.5 \times 10^{-4} \text{dL/g}$  and 0.766, respectively for the THF-PVC system at  $25^\circ\text{C}$ <sup>24</sup>.

The action of ZnS nanocrystals on PVC matrix was assessed by comparison of the Degradation Index (DI) for irradiated samples using Equation 3.

$$DI = \left( \frac{M_{v0}}{M_v} \right) - 1 \quad (3)$$

where  $M_{v0}$  and  $M_v$  are the Viscosity Average Molar Mass before and after gamma irradiation, respectively. DI is obtained from viscosity analysis and reflects the number of main chain scissions per original molecule after irradiation<sup>25</sup>.

### 2.4 Irradiation of samples

PVC and PVC/ZnS films were exposed to gamma radiation from a non-attenuated  $^{60}\text{Co}$  source (Gammacell GC220 Excel irradiator - MDS Nordion, Canada), at 25 kGy dose in air, dose rate of 2.66 kGy/h, at room temperature ( $\approx 27^\circ\text{C}$ ).

### 2.5 Free radical scavenging action of ZnS nanocrystals

The free radical scavenging action assessment was grounded on DPPH (2,2-diphenyl-1-(2,4,6-trinitrophenyl)-hydrazyl) radical strong visible light absorption, characterized by an intense violet coloration due to the presence of unpaired electrons<sup>27</sup>. In the presence of radical scavengers, DPPH solution color fades, leading to a stoichiometric discoloration in relation to the number of reduced DPPH radicals. In brief, 2.4 mg of DPPH were dissolved in 10 mL of the absolute ethanol and 1.2 mg of ZnS nanocrystals (equivalent to a concentration of 0.7 wt% in PVC matrix) were mixed with the DPPH solution under vigorous stirring at room temperature ( $\approx 27^\circ\text{C}$ ) for 30 minutes. Free radical scavenging action of ZnS was evaluated through the decrease in DPPH solution visible absorption at 515 nm, using BHT (2,6-bis(1,1-dimethylethyl)-4-methylphenol) as a positive control.

### 2.6 Mechanical properties

Tensile properties of the PVC and PVC/ZnS were determined according to ASTM D-882-12<sup>28</sup> using an Instron machine EMIC, DL-500 N. Results were expressed as the mean value of four samples. The tests took place at room

**Table 1.** Equations used for viscosity measurements.

Viscosity measurement	Equation	Description	Reference
Relative viscosity ( $\eta_{rel}$ )	$\eta_{rel} \approx v/v_0$	$v$ and $v_0$ are the cinematic viscosities on the polymer solution and the solvent, respectively	23
Specific viscosity ( $\eta_{sp}$ )	$\eta_{sp} = \eta_{rel} - 1$	-	23
reduced viscosity ( $\eta_{red}$ )	$\eta_{red} = \eta_{sp}/C$	$C$ is solution concentration (0.6 g/dL)	23
Intrinsic viscosity [ $\eta$ ]	$[\eta] = \frac{1}{C} \sqrt{2(\eta_{sp} - \ln \eta_{rel})}$	-	26

temperature. Assays were performed under the following conditions: load cell of 500 N, crosshead speed of 2 mm/min, and sample dimension of 2.5 x 7.5 x 0.12 cm.

### 2.7 FTIR characterization

Fourier Transform Infrared (FTIR) spectra were obtained using a Jasco 4600 FTIR Spectrometer (Tokyo, Japan), equipped with an attenuated total reflection accessory (ATR ProOne, ZnSe crystal), operating at a 4  $\text{cm}^{-1}$  resolution, ranging from 400 to 4000  $\text{cm}^{-1}$  with 75 scans/spectrum.

### 2.8 Principal Component Analysis (PCA) of FTIR spectra

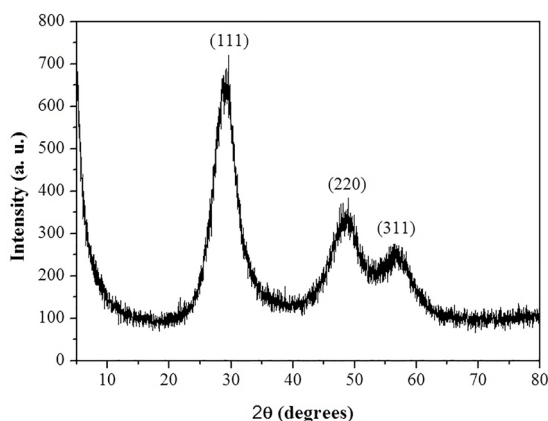
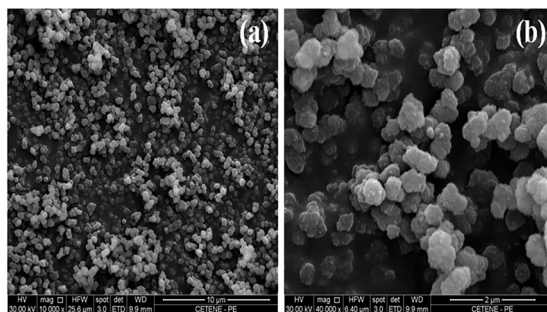
PCA was performed using PVC and PVC/ZnS FTIR data in the 2000 $\text{cm}^{-1}$  - 500 $\text{cm}^{-1}$  wavelength range. FTIR spectra were exported in the JCAMP-DX format and treated with The Unscrambler<sup>(r)</sup> 9.7 software (CAMO Software AS, Norway). Spectra were made in quintuplicate. Raw data were normalized and modelled to determine variable scores and assess which components are able to explain major variabilities in the spectroscopic data matrix.

## 3. Results and Discussion

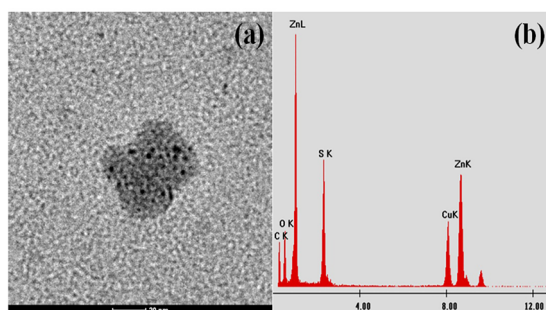
### 3.1 ZnS nanocrystals characterization

Fast and simple sonochemical method was used to obtain ZnS nanocrystals from  $\text{C}_4\text{H}_6\text{O}_4\text{Zn} \cdot \text{H}_2\text{O}$  and thioacetamide, as evidenced by XRD analysis. X-ray diffractogram of sonochemically produced ZnS is shown in Figure 1. The diffraction peaks at  $2\theta$  values of 29.44°, 48.46° and 56.69° match well (111), (220), and (311) crystalline planes of cubic ZnS, respectively. The significant broadening of the diffraction peaks may be attributed to small ZnS crystallite sizes. The crystal size estimated from the intense  $2\theta = 29.44^\circ$  (111) XRD peak is about 2 nm, according to the Debye-Scherrer equation (Equation 1). These results confirm the formation of ZnS with good crystallinity in cubic (sphalerite) phase and agree with literature results<sup>29</sup>.

ZnS nanoparticles morphology was analyzed by SEM experiments (Figure 2). It was observed that the ZnS crystals form spherical aggregates around 600 nm. Nanoparticles agglomeration is expected as their high surface area make them thermodynamically unstable. Nanoparticle close contact reduces total exposed area, decreasing energy surface, therefore, stabilizing the particles<sup>30,31</sup>.

**Figure 1.** XRD pattern of ZnS nanoparticles.**Figure 2.** SEM micrographs for ZnS nanoparticles in a) 10,000x and b) 40,000x.

TEM analysis evidenced ZnS crystals with diameters ranging from 2 to 3 nm (Figure 3a). Qualitative EDS analysis revealed S and Zn peaks, further confirming the samples identity, as shown in Figure 3b.

**Figure 3.** a) TEM micrograph and b) EDS result for ZnS nanoparticles.

### 3.2 Radiostabilizing action of ZnS nanocrystals in PVC matrix

When PVC was exposed to gamma radiation at 25kGy, its Mv decreased and DI value found was 0.094 as shown in Table 2. These results suggest the predominance of main chain scissions upon irradiation, in agreement with literature reports about gamma radiation effects on PVC matrix<sup>32-34</sup>. However, minor effect in Mv occurred in irradiated PVC/ZnS films with increase of ZnS concentration up to 0.7wt%, with calculated DI = 0.024. These results evidenced around 74% less scissions per original molecule of PVC, leading to an effective radiolytic stabilization of the polymer matrix owed to the presence of ZnS nanocrystals. In addition, a decrease in ZnS stabilizing action occurred when its concentration reached 1.00 %wt. This is a rather common effect in polymer-additives systems as optimum additive concentration is overreached<sup>13,14</sup>.

**Table 2.** Viscosity results for PVC and PVC/ZnS at different concentrations.

ZnS concentration (% wt)	DI	Protection(%)
0	0.094	----
0.1	0.091	3.52
0.3	0.086	8.69
0.5	0.073	22.16
0.7	0.024	74.56
1.0	0.102	Zero

To the best of our knowledge, no information about the use of ZnS nanocrystals in radiolytic stabilization of polymers has been published, so far. Consequently, many aspects of the radiostabilizing mechanism remain unclear. In this work, ZnS nanocrystals are suggested to play an important role in PVC radiostabilization. It is well known that gamma rays can break covalent bonds in PVC molecule to directly produce radicals, leading to further PVC degradation<sup>35,36</sup>. Nevertheless, our attempts to detect radical scavenging activities in ZnS nanocrystals using DPPH test were not successful. Intense violet coloration of DPPH solution (Figure 4a) showed no appreciable discoloration after ZnS nanocrystals addition in concentration equivalent to 0.7 wt% used in the PVC matrix. For comparison, BHT, the positive control, exhibited radical scavenging capacity by discoloring DPPH solution (Figure 4c).

Probably, ZnS acts as a quencher, deactivating excited states species formed during irradiation. Such activity was reported before in sulfur-containing substances, e.g. hydrogen sulfide, ethanethiol or diethylsulfide<sup>37</sup>, however further work is required to elucidate the processes involved in the stabilizing action of ZnS nanocrystals in PVC matrix.

### 3.3 PVC/ZnS films characterization

SEM images of PVC/ZnS at studied concentrations showed similar behavior with homogeneous dispersion of nanoparticles in the polymer matrix. Figure 5 shows SEM images of PVC and PVC/ZnS film containing 0.7 wt% of ZnS presenting randomly distributed nanoparticle aggregates. The small ZnS size may induce aggregation of the nanoparticles to energetically stabilize PVC/ZnS system, thus lowering the homogeneity of particle distribution. SEM images of irradiated nanocomposites presented similar features as non-irradiated nanocomposites and are not shown in this paper.

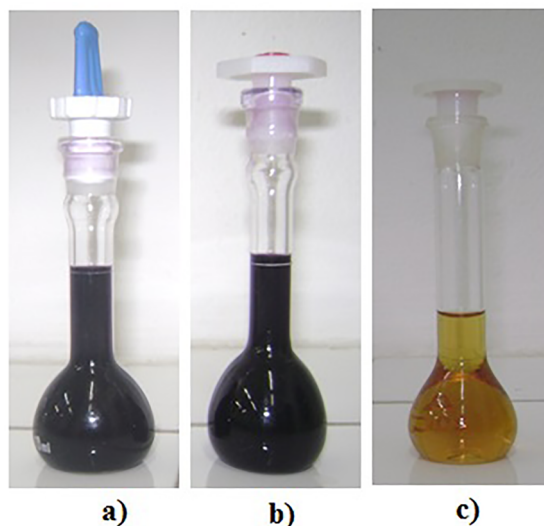


**Figure 4.** DPPH radical results: a) DPPH solution, b) DPPH+ZnS and c) DPPH+BHT.

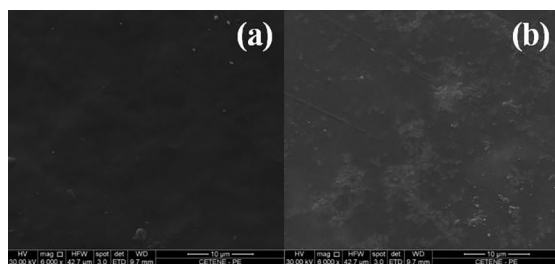


**Figure 5.** SEM micrographs of a) PVC film and b) PVC/ZnS film (0.7%wt).

FTIR spectroscopy was used to detect and identify the presence of intermolecular interactions between PVC molecules and ZnS. Figure 6 shows FTIR spectra of PVC and PVC/ZnS (0.7wt%) for non-irradiated and irradiated films in the 4000-500  $\text{cm}^{-1}$  wavenumber region. C=O stretching vibration in 1717  $\text{cm}^{-1}$  is typical of ketone/aldehyde<sup>38</sup>, and may be attributed to residual MEK solvent used in the production of samples. Characteristic PVC vibrational modes can be

classified in five types<sup>38,39</sup>: a) C-Cl stretching 600-700  $\text{cm}^{-1}$  range ; b) C-C stretching vibrations in the 900-1200  $\text{cm}^{-1}$  range c)  $\text{CH}_2$  deformation in the 1300-1350 $\text{cm}^{-1}$  range d) C-H rocking 1240 - 1260 and *trans*- C-H wagging 950 - 960  $\text{cm}^{-1}$  range. All spectra exhibited peaks within the expected range. However, shifts in C-Cl stretching band were found in PVC/ZnS spectra when compared to PVC data. PVC peak at 692  $\text{cm}^{-1}$  is shifted to 681  $\text{cm}^{-1}$  in PVC/ZnS for non-irradiated samples. On the other hand, PVC peak at 692  $\text{cm}^{-1}$  is shifted to 688  $\text{cm}^{-1}$  in irradiated samples, but no significant shifts were found between irradiated PVC/ZnS samples. Such changes in C-Cl stretching peaks suggest molecular interactions between PVC chlorine atoms and ZnS, and might shed some light on the radiolysis protection mechanism, since the loss of chlorine radicals is the main initiation step for PVC radiolysis<sup>40</sup>.

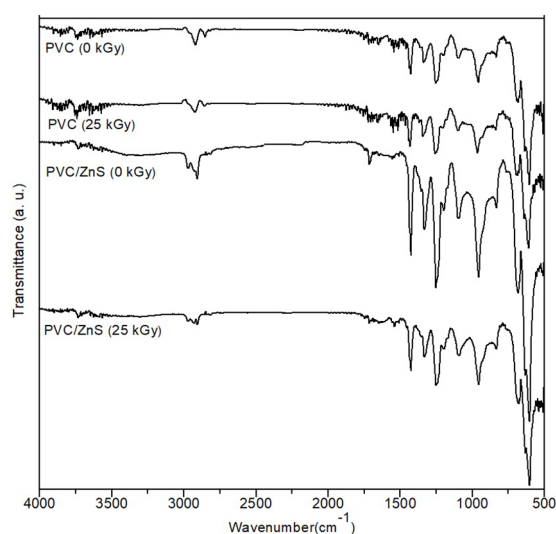


**Figure 6.** FT-IR spectra for PVC and PVC/ZnS (0.7%wt) irradiated and unirradiated.

Further evidences on intermolecular interactions between PVC and ZnS nanocrystals could be assessed by PCA analysis of FTIR spectra. Figure 7 shows that PCA for PVC and PVC/ZnS were separated into two distinct groups. This result means that there were differences between the systems and suggest specific PVC - ZnS interactions. The loading spectra showed more relevant changes for C-Cl peak in the PVC/ZnS sample. The percentages of variance explained by PC1 and PC2 were 98% and 1%, respectively. PCA of PVC irradiated samples revealed a tendency of separation in two distinct vertical groups (Figure 8). Loading data also suggest the most striking differences in the vibrations of the C-Cl group with slight chemical shift, probably due to irradiation effects. However, for PVC/ZnS samples it is possible to observe that, although there is a trend of vertical separation of groups, the samples data distribution are very close; which means that there are small differences in the vicinity of PVC

C-Cl bonds. These results reinforce the idea of PVC chlorine atom - ZnS interaction as a possible stabilization pathway, which may explain a molecular protection greater than 70% upon the addition of ZnS 0.7 %wt.

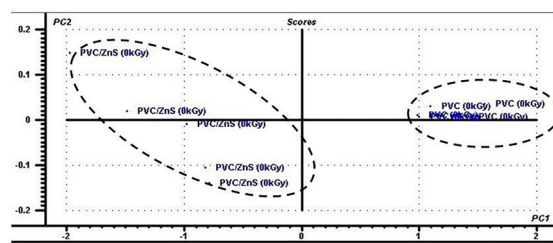


**Figure 7.** Score plots of PC1 x PC2 of PVC and PVC/ZnS films.

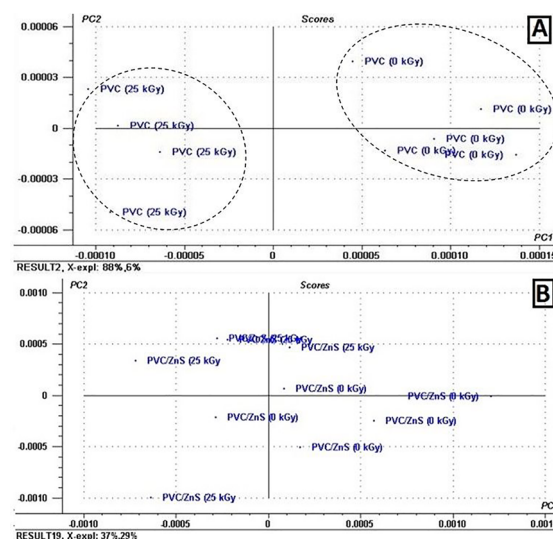


**Figure 8.** Score plots of PC1 x PC2 of irradiated systems for a) PVC and b) PVC/ZnS.

### 3.4 Mechanical properties

The influence of ZnS nanocrystals on PVC mechanical properties was investigated through tension tests. The results of tensile strength (TS) and Young's modulus (Ym) for PVC and PVC/ZnS (0.7wt%) are summarized in Table 3 for both irradiated and non-irradiated samples. The mean values of the mechanical properties were statistically compared by Student's t-test, with a significance level of 5% ( $p < 0.05$ ).

The tensile strength expresses the maximum strength of the material when under tension<sup>41</sup>. By the Student's t-test it was observed that ZnS incorporation causes a decrease around 10% in tensile strength when compared to non-irradiated samples. In relation to the Young's modulus, the values found for PVC/ZnS decreased 25% when compared to Ym values of PVC. Thus, the incorporation of ZnS in the PVC matrix resulted in a less resistant material by decreasing of tensile strength value and a less rigid material by decreasing Young's modulus. As PVC is a rigid polymer, this change in stiffness is very positive when the films are intended for

**Table 3.** Mechanical results obtained for PVC and PVC/ZnS.

	Dose (kGy)	YM (MPa)	TS (MPa)
PVC	0	2,672.38 ± 104.81 <sup>a</sup>	44.42 ± 1.34 <sup>a</sup>
	25	1,621.80 ± 128.73 <sup>b</sup>	33.91 ± 2.55 <sup>b</sup>
PVC/ZnS	0	2,000.64 ± 58.33 <sup>c</sup>	37.09 ± 2.54 <sup>c</sup>
	25	2,056.81 ± 35.46 <sup>c</sup>	40.09 ± 1.90 <sup>c</sup>

Means with the same letter in the same column do not differ with  $p < 0.05$  for the Student's t-test.

applications which require higher flexibility, such as medical use materials.

PVC shows intermolecular dipole-dipole attraction between the electron-rich chlorine atom of a PVC chain (negative pole) and electron-deficient chlorine-bonded carbon at a nearby PVC molecule (positive pole). New C-Cl<sup>-</sup>Zn interactions formed in the presence of ZnS, as suggested by PCA analysis (Figure 7) might weaken interchain interactions, causing increase in macromolecular mobility and decrease in the density of entanglement points<sup>32,38</sup>.

On the other hand, PVC sample irradiated at 25kGy exhibited lower TS and Ym values when compared to non-irradiated PVC samples (Table 3). As viscosity analysis revealed radiolysis with main chain scissions at 25kGy dose (Table 2), a decrease in the density of entanglements points is expected as a consequence of shorter PVC molecules after irradiation. However, no statistically significant changes were found for irradiated PVC/ZnS. These results are explained by stabilizing action of ZnS on PVC matrix and agree with viscosity measurements.

## 4. Conclusions

ZnS nanoparticles were synthesized through sonochemical method as a nanocrystalline powder. The dispersion of these nanostructures in PVC matrix at low concentration (0.7 wt%) resulted in radiolytic stabilization by decreasing degradation index from 0.094 to 0.024. PCA analysis performed in FTIR spectra of PVC films containing ZnS indicated C-Cl<sup>-</sup>ZnS interactions. Such interactions might have contributed to improved mechanical properties of PVC/ZnS systems. Our findings might have paved the way to a new line of affordable additive nanoparticles for radiolytic stabilization and mechanical improvement of PVC.

## 5. Acknowledgments

We would like to thank CNPq-Brazil for financial support and BRASKEM-Brazil for PVC samples.

## 6. References

- Hanemann T, Szabó DV. Polymer-Nanoparticle Composites: from Synthesis to Modern Applications. *Materials*. 2010;3(6):3468-3517.

- Li P, Chen X, Zeng JB, Gan L, Wang M. Enhancement of the interfacial interaction between poly(vinyl chloride) and zinc oxide modified reduced graphene oxide. *RSC Advances*. 2016;6(7):5784-5791.
- Chen CH, Teng CC, Yang CH. Preparation and Characterization of rigid poly(vinyl chloride)/MMT nanocomposites. *Journal of Polymer Science: Part B: Polymer Physics*. 2005;43(12):1465-1474.
- Fang X, Zhai T, Gautam UK, Li L, Wu L, Bando Y, et al. ZnS nanostructures: From synthesis to applications. *Progress in Materials Science*. 2011;56(2):175-287.
- Murugadoss G. Synthesis and photoluminescence properties of zinc sulfide nanoparticles doped with copper using effective surfactants. *Particuology*. 2013;11(5):566-573.
- Kolahi S, Farjami-Shayesteh S, Azizian-Kalandaragh Y. Comparative studies on energy-dependence of reduced effective mass in quantum confined ZnS semiconductor nanocrystals prepared in polymer matrix. *Materials Science in Semiconductor Processing*. 2011;14(3-4):294-301.
- Ogata T, Hirakawa N, Nakashima Y, Kuwahara Y, Kurihara S. Fabrication of polymer/ZnS nanoparticle composites by matrix-mediated synthesis. *Reactive & Functional Polymers*. 2014;79:59-67.
- Osuntokun J, Ajibade PA. Structural and Thermal Studies of ZnS and CdS Nanoparticles in Polymer Matrices. *Journal of Nanomaterials*. 2016;2016:3296071.
- Tiwari A, Dhoble SJ. Stabilization of ZnS nanoparticles by polymeric matrices: syntheses, optical properties and recent applications. *RSC Advances*. 2016;6(69):64400-64420.
- Harifi T, Montazer M. A review on textile sonoprocessing: a special focus on sonosynthesis of nanomaterials on textile substrates. *Ultrasonics Sonochemistry*. 2015;23:1-10.
- Suslick KS, Choe SB, Cichowlas AA, Grinstaff MW. Sonochemical synthesis of amorphous iron. *Nature*. 1991;353:414-416.
- Xu H, Zeiger BW, Suslick KS. Sonochemical synthesis of nanomaterials. *Chemical Society Reviews*. 2013;42(7):2555-2567.
- Albuquerque MCC, Garcia OP, Aquino KAS, Araujo PLB, Araujo ES. Stibnite Nanoparticles as a New Stabilizer for Poly (Methyl Methacrylate) Exposed to Gamma Irradiation. *Materials Research*. 2015;18(5):978-983.
- Garcia OP, Albuquerque MCC, Aquino KAS, Araujo PLB, Araujo ES. Use of Lead (II) Sulfide Nanoparticles as Stabilizer

- for PMMA Exposed to Gamma Irradiation. *Materials Research*. 2015;18(2):365-372.
15. Goharshadi EK, Hadadian M, Karimi M, Azizi-Toupkanloo H. Photocatalytic degradation of reactive black 5 azo dye by zinc sulfide quantum dots prepared by a sonochemical method. *Materials Science in Semiconductor Processing*. 2013;16(4):1109-1116.
  16. Xu JF, Ji W, Lin JY, Tang SH, Du YW. Preparation of ZnS nanoparticles by ultrasonic radiation method. *Applied Physics A*. 1998;66(6):639-641.
  17. She YY, Yang J, Qiu K. Synthesis of ZnS nanoparticles by solid-liquid chemical reaction with ZnO and Na<sub>2</sub>S under ultrasonic. *Transactions of Nonferrous Metals Society of China*. 2010;20(Suppl 1):s211-s215.
  18. Zhao Z, Geng F, Cong H, Bai J, Cheng H. A simple solution route to controlled synthesis of ZnS submicrospheres, nanosheets and nanorods. *Nanotechnology*. 2006;17(18):4731-4735.
  19. Nanda J, Sapra S, Sarma DD, Chandrasekharan N, Hodes G. Size-Selected Zinc Sulfide Nanocrystallites: Synthesis, Structure, and Optical Studies. *Chemistry of Materials*. 2000;12(4):1018-1024.
  20. Biswas S, Kar S, Chaudhuri S. Synthesis and Characterization of Zinc Sulfide Nanostructures. *Synthesis and Reactivity in Inorganic, Metal-Organic, and Nano-Metal Chemistry*. 2006;36(1):33-36.
  21. Silva FF, Aquino KAS, Araújo ES. Effects of gamma irradiation on poly(vinyl chloride)/polystyrene blends: Investigation of radiolytic stabilization and miscibility of the mixture. *Polymer Degradation and Stability*. 2008;93(12):2199-2203.
  22. Silva WB, Aquino KAS, Vasconcelos HM, Araújo ES. Influence of copper chloride and potassium iodide mixture in poly(vinyl chloride) exposed to gamma irradiation. *Polymer Degradation and Stability*. 2013;98(1):241-245.
  23. Guillet J. *Polymer Photophysics and Photochemistry*. New York: Cambridge University Press; 1985.
  24. Brandrup J, Immergut EH, eds. *Polymer Handbook*. New York: John Wiley Sons; 1989.
  25. Charlesby A. *Atomic Radiation and Polymers*. New York: Pergamon Press; 1960.
  26. Solomo OF, Ciută IZ. Détermination de la viscosité intrinsèque de solutions de polymères par une simple détermination de la viscosité. *Journal of Applied Polymer Science*. 1962;6(24):683-686.
  27. Mathiesen L, Malterud KE, Sund RB. Hydrogen Bond Formation as Basis for Radical Scavenging Activity: A Structure-Activity Study of C-Methylated Dihydrochalcones from Myrica Gale and Structurally Related Acetophenones. *Free Radical Biology & Medicine*. 1997;22(1-2):307-311.
  28. ASTM International. *ASTM D882-12 - Standard Test Method for Tensile Properties of Thin Plastic Sheeting*. West Conshohocken: ASTM International; 2012.
  29. Nanev C, Iwanov D. Direct synthesis of epitaxial zinc sulphide layers on zinc single-crystal substrates. *Thin Solid Films*. 1976;35(2):155-163.
  30. Hotze EM, Phenrat T, Lowry GV. Nanoparticle Aggregation: Challenges to Understanding Transport and Reactivity in the Environment. *Journal of Environmental Quality*. 2010;39(6):1909-1924.
  31. Zemb T, Kunz W. Weak aggregation: State of the art, expectations and open questions. *Current Opinion in Colloid & Interface Science*. 2016;22:113-119.
  32. Vinhas GM, Souto-Maior RM, Almeida YMB, Neto BB. Radiolytic degradation of poly(vinyl chloride) systems. *Polymer Degradation and Stability*. 2004;86(3):431-436.
  33. Vinhas GM, Souto Maior RM, Almeida YMB. Radiolytic degradation and stabilization of poly(vinyl chloride). *Polymer Degradation and Stability*. 2004;83(3):429-433.
  34. Mendizabal E, Cruz L, Jasso CF, Burillo T, Davin VT. Radiation crosslinking of highly plasticized PVC. *Radiation Physics and Chemistry*. 1996;47(2):305-309.
  35. Lee EH, Rao GR, Mansur LK. LET effects on cross-linking and scission mechanism of PVC during irradiation. *Radiation Physics and Chemistry*. 1999;55(3):293-305.
  36. Von Cottrel TL. *The Strengths of Chemical Bonds*. London: Butterworths; 1954.
  37. Lendvay G, Bérces T. Radical Scavenging and excited state quenching efficiency of additives in the photochemistry of acetone. *Journal of Photochemistry and Photobiology, A: Chemistry*. 1987; 40: 31-45.
  38. Ramesh S, Leen KH, Kumutha K, Arof AK. FTIR studies of PVC/PMMA blend based polymer electrolytes. *Spectrochimica Acta Part A: Molecular and Biomolecular Spectroscopy*. 2007;66(4-5):1237-1242.
  39. Rajendran S, Uma T. Effect of ZrO<sub>2</sub> on conductivity of PVC-LiBF<sub>4</sub>-DBP polymer electrolytes. *Materials Letters*. 2000;44(3-4):208-214.
  40. Colombani J, Labele V, Jousset-Dubien C, Périchaud A, Raffi J, Kister J, et al. High doses gamma radiolysis of PVC: Mechanisms of degradation. *Nuclear Instruments and Methods in Physics Research Section B: Beam Interactions with Materials and Atoms*. 2007;265:238-244.
  41. Lipatov YS. *Polymer Reinforcement*. Toronto: ChemTec Publishing; 1995.